3D Echocardiographic Imaging and Modeling: Towards the Patient-Specific Virtual Mitral Valve

Emiliano Votta[a], Marco Stevanella[a], Laura Fusini[a,b], Federico Veronesi[c], Gloria Tamborini[b], Mauro Pepi[b], Francesco Maffessanti[a,b], Francesco Alamanni[c], Alberto Redaelli[a], Enrico G Caiani[a]

[a] Biomedical Engineering Department, Politecnico di Milano, Milano, Italy
[b] Centro Cardiologico Monzino IRCCS, Milan, Italy
[c] Department of Cardiovascular Sciences, Università degli Studi di Milano, Milan, Italy

Abstract

Finite element models (FEMs) have been already widely used to analyze mitral valve (MV) biomechanics. Recently, strategies to implement patient-specific, image-based FEMs of the MV were proposed, improving their realism. In particular, we proposed to implement MV FEMs from real time 3D transthoracic echocardiographic imaging. To allow a future clinical use of this approach as a support tool for MV surgical planning, we applied it to three healthy and three regurgitant MVs, to test for its capacity in discriminating between physiological and pathological MV function, in realistically capturing location and extent of the regurgitating areas, and in quantifying the biomechanical anomalies associated to MV regurgitation. MV FEMs proved able to simulate both physiological and pathological MV function, thus confirming the ability of this promising approach in potentially being applied as support tool for surgical planning.

1. Introduction

The mitral valve (MV) separates the left atrium and the left ventricle; in physiological conditions it guarantees the unidirectional flow from the former to the latter during ventricular diastole, while preventing backward flow during systole. This function highly depends on the dynamics and the interaction of the substructures composing the MV: i) the two valve leaflets, ii) the mitral annulus (MA), which surrounds the valve orifice and acts like an active sphincter, iii) the chordae tendineae, which connect the leaflets to the ventricular myocardium, converging on iv) two papillary muscles (PMs), which contract and move dynamically.

MV pathologies have a high prevalence and require surgical intervention, the preferential approach being surgical repair. In the last decade, repair techniques have become increasingly effective, but at same time more complex. Their conceiving and application are currently based on the empirical experience of surgeons, and can be improved by means of design tools capable of predicting the effects of the intervention. Among these, finite element models (FEMs) have been demonstrated to be very powerful, as they allow for the detailed and quantitative biomechanical analysis of the MV in a variety of scenarios, including post-operative conditions following a hypothetical surgical procedure, through computational simulations. Since the 90s, MV FEMs have been proposed to better understand the physiological MV function, to elucidate the mechanisms underlying MV pathologies, and to assess the effects of surgical devices and repair [1-2]. In this time-frame, FEMs have become more and more realistic, and methods to generate patient-specific MV FEMs directly from clinical imaging data have been proposed [3-5]. Once properly refined and validated, these methods would not only allow a better understanding of mechanisms of general validity, but would also be helpful as supporting tools for surgical planning. In this scenario, we recently proposed an approach to develop patient-specific MV FEMs from non-invasive transthoracic (TTE) real time 3-D echocardiography (RT3DE), and successfully tested it on a single healthy MV [5].

Aim of this work was to apply our method on both healthy and regurgitant MVs with degenerative prolapse (MVP), to test its capability to i) capture the location and severity of the prolapse in pathological valves, ii) to discriminate between physiological and pathological MV biomechanics, and iii) to validate FEM morphology in MVP by comparison with transesophageal (TEE) RT3DE data.

2. Methods

Three healthy volunteers (NLs) and three patients with MV organic prolapse (MVPs) undergoing early surgery

(with ejection fraction >55%) were studied. Figure 1 shows a schematization of the whole process. All the subjects underwent TTE RT3DE; the corresponding datasets were processed using custom software to detect and track the MA and the PMs [6]. MV FEMs, inclusive of these patient-specific morphological information, were semi-automatically generated via in home Python code. FEMs were used to simulate MV function from end-diastole (ED) to peak systole (PS) through of the commercial numerical solver ABAQUS/Explicit 6.9-1 (SIMULIA, Dassault Systèmes). FEMs results regarding NLs and MVPs were compared.

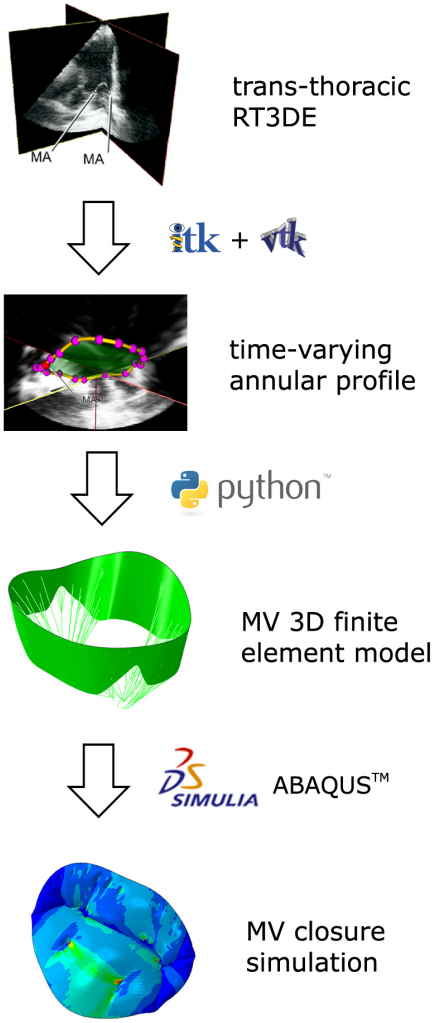

Figure 1. Workflow used to implement and run patient-specific MV FEMs based on TTE RT3DE.

2.1. Echocardiographic image acquisition

Both TTE and TEE RT3DE imaging were performed (iE33, Philips, Andover, MA) from the apical window using a fully sampled matrix-array transducer (X3), with the subject in the left lateral decubitus position. RT3DE datasets were acquired using the wide-angled mode at high frame rate (31 Hz), wherein 8 wedge-shaped subvolumes were obtained during 8 cardiac cycles during a single breath hold with ECG gating.

2.2. RT3DE image processing

The TTE RT3DE data were analyzed using previously developed custom software to semi-automatically detect and track the MA throughout the cardiac cycle, and to identify the PMs tips [6]. Briefly, on the ED frame, 18 long-axis cut planes evenly rotated around the center of the MA (10° step) were displayed to complete the initialization procedure. On each plane, the operator selected 2 points, one on each side of the MA. Subsequently, the positions of each initialized point were automatically tracked frame-by-frame in 3D space, using optical flow and region-based matching techniques. The automatically tracked points were displayed in each frame to verify their position, and manual corrections were performed when necessary. To identify the PM tips, on the ED frame the dataset was analyzed by rotating the cut plane around the MA center, until the tip of each PM was best visualized. On the selected plane, the operator defined a point at the position of the PM tip. Moreover, on the ED frame additional information regarding leaflets orientation in space was gathered, measuring their tilting in an apical 4-chamber cut plane.

2.3. MV geometrical modeling

The ED configuration was chosen as the reference. The MV FEM geometrical model was implemented defining i) the annular profile, by Fourier interpolation of the 36 points selected on the MA in the ED frame. The continuous profile was than sampled into ~400 nodes that provided the seeding for the mesh to be defined on leaflets surface; ii) PM tips, defined as two circumferences (3 mm diameter) centered in the two points selected in the ED frame; iii) the leaflets, whose profile, based on ex-vivo data from the literature [7], was adapted to the subject's annular size and spatial orientation. The anterior and posterior leaflets were assumed 1.32 and 1.26 mm thick, respectively, and two transitional commissural zones with a thickness of 1.29 mm were also identified. Leaflets were discretized using 3-nodes shell elements; iv) a complete chordal apparatus, where the number of chordae, the corresponding branched structure and insertion sites on the leaflets were defined in accordance to ex vivo findings [8]. Constant cross-sectional area values of 0.4, 1.15 and 0.79 mm^2 were used for marginal, strut and basal chordae, respectively [9].

2.4. MV tissue mechanical properties

All tissues were assumed non-linear and elastic. Their mechanical response was described by means of proper strain energy potentials. Leaflets anisotropic response was accounted for by means of a Fung-like strain energy potential [10]. Chordae tendineae response was assumed isotropic. A second order polynomial strain energy potential was used for marginal chordae; a fifth order Ogden strain energy function was used for strut and basal chordae. The constitutive parameters were defined via mean-square interpolation of literature data [9,11].

2.5. Boundary conditions

The dynamic contraction of MA and PMs was modelled imposing proper nodal displacements. A continuous MA profile was obtained from each frame for the TTE RT3DE data, interpolating the 36 tracked points. The resulting continuous profile was sampled as for the ED frame, and nodal displacements were calculated. The motion of PMs tips was estimated from in vivo data obtained in animal models [12]. A physiological time-dependent transvalvular pressure drop, up to 120 mmHg, was applied on the leaflets.

2.6. TEE RT3DE quantification

For the three MVP patients, TEE RT3DE images acquired intra-operatively were transferred to a workstation for off-line analysis using the MVQ software, part of the QLab suite (Philips Medical Systems). The configurations of the MV annulus and leaflets at PS was obtained, and used as comparison with the one computed through the FEMs to see if the model was able to correctly describe the prolapse position.

3. Results and discussion

For NLs, the computed MV dynamics and coaptation were consistent with experimental findings; coaptation involved the leaflet's rough zone, and was complete for pressures of 15÷25 mmHg [13]. Still, a non-physiological bulging of the anterior leaflet was obtained, whose complex compound shape was not reproduced.

For MVPs, the computed MV configuration at PS was characterized by leaflet prolapse and incomplete coaptation. FEMs were able to reproduce with good approximation the extent and the position of the prolapsing tissue and of the regurgitant areas, when visually compared to the QLab configuration (figure 2).

Notable differences between MVPs and NLs were observed in terms of computed leaflet stresses, MA forces and PM tensions at PS. Namely, in MVPs an abnormal stress increase was found in the annular region of the prolapsing cusps, while marked peak stresses in MVPs were detected next to the fibrous trigones (450÷500 kPa vs 230÷360 kPa in NLs, figure 3).

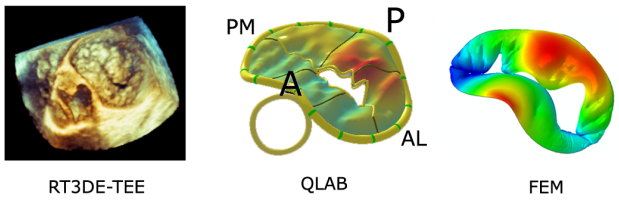

Figure 2. Example of MVP at PS, as seen by TEE RT3DE (left), as reconstructed by QLab (center), and as computed by the FEM (right). Color-coded contour maps represent the signed distance from the annular plane.

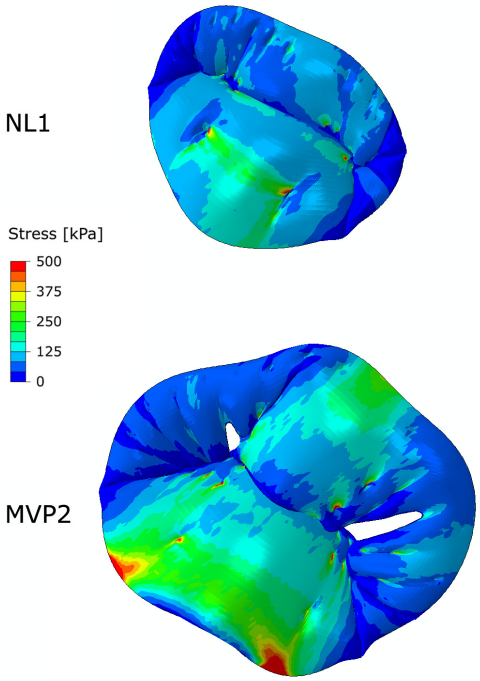

Figure 3. Leaflets maximum principal stresses in representative NL and MVP subjects.

As regards MA reaction forces at PS, in MVPs their regional distribution maintained the same pattern as NLs, with extremely low values at the commissures and paracommissures, and peak values at the fibrous trigones. However, their average force over the anterior and posterior portion of the MA increased from 0.05÷0.10 to 0.14÷0.27 N and from 0.03÷0.04 to 0.08÷0.10 N, respectively (figure 4). A similar increase was observed in PM tension magnitude at PS; PM force averaged over the two PMs was 4.13÷5.89 N in NLs, and increased up to 7.63÷11.05 N in MVPs.

Compared to NLs, our results in MVPs show that the increases in leaflet stresses at the fibrous trigones, in MA

reaction force peak values, and PM tension are consistent, and reflect the fact that the three mentioned MV substructures are contiguous, and transmit the mechanical loads due to ventricular pressure as in a closed loop.

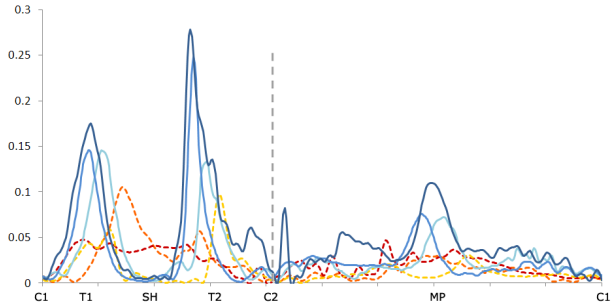

Figure 4. Local annular forces [N] for the six MVs. Dashed and continuous lines refer to NLs and MVPs, respectively. C1,C2=commissures; SH=saddle-horn; T1,T2=trigones; MP=posterior midpoint. Dashed grey line separates anterior (left) from posterior annulus (right).

4. Conclusions

MV FEMs based on non-invasive TTE RT3DE imaging proved able to simulate physiological and pathological MV function.

When used to simulate the systolic function of MVs with organic prolapse, the proposed modeling strategy proved capable of mimicking with good approximation the real valve closure, capturing the main features of the pathology. Also, the morphological configuration at PS was comparable with the one observed intra-operatively using TEE RT3DE. Moreover, it allowed to discriminate between physiological and pathological patterns of biomechanical variables over the MV substructures.

Thus, our modeling approach fulfilled two crucial preconditions to move towards its application to the prediction of hypothetical post-operative scenarios, and thus to develop a support tool for the surgical planning.

5. Acknowledgements

This work was supported by the Italian Ministry of Research under the PRIN 2007 program as part of the SurgAid project (www.surgaid.org) and by Regione Lombardia and CILEA Consortium through a LISA Initiative (Laboratory for Interdisciplinary Advanced Simulation) 2010 grant (http://lisa.cilea.it).

6. References

[1] Kunzelman KS, Einstein DR, Cochran RP. Fluid-structure interaction models of the mitral valve: function in normal and pathological states. Philos. Trans R Soc Lond B Biol Sci 2007;362:1393-1406.

[2] Votta E, Maisano F, Bolling SF, Alfieri O, Montevecchi FM, Redaelli A. The Geoform disease-specific annuloplasty system: a finite element study. Ann Thorac Surg 2007;84:92-101.

[3] Wenk JF, Zhang Z, Cheng G, Malhotra D, Acevedo-Bolton G, Burger M, Suzuki T, Saloner DA, Wallace AW, Guccione JM, Ratcliffe MB. First finite element model of the left ventricle with mitral valve: insights into ischemic mitral regurgitation. Ann Thorac Surg. 2010;89(5):1546-1553.

[4] Ionasec RI, Voigt I, Georgescu B, Wang Y, Houle H, Vega-Higuera F, Navab N, Comaniciu D. Patient-specific modeling and quantification of the aortic and mitral valves from 4-D cardiac CT and TEE. IEEE Trans Med Imaging. 2010;29(9):1636-1651.

[5] Votta E, Caiani E, Veronesi F, Soncini M, Montevecchi FM, Redaelli A. Mitral valve finite-element modeling from ultrasound data: A pilot study for a new approach to understand mitral function and clinical scenarios. Philos Transact A Math Phys Eng Sci 2008;366 (1879):3411-3434.

[6] Veronesi F, Corsi C, Sugeng L, Caiani EG, Weinert L, Mor-Avi V, Cerutti S, Lamberti C, Lang RM. Quantification of mitral apparatus dynamics in functional and ischemic mitral regurgitation using real-time 3-dimensional echocardiography. J Am Soc Echocardiogr 2008;21:347-54.

[7] Kunzelman KS, Cochran RP, Verrier ED, Eberhart RC. Anatomic basis for mitral valve modeling. J. Heart Valve Dis 1994;3:491-496.

[8] Lam JHC, Ranganathan N, Silver MD. Morphology of the human mitral valve. I. Chordae tendinae: a new classification. Circulation 1970;41:449-458.

[9] Kunzelman, K. S., and R. P. Cochran. Mechanical properties of basal and marginal mitral valve chordae tendineae. ASAIO Trans 1990;36(3):M405–M408.

[10] Prot V, Haaverstad R, Skallerud B. Finite element analysis of the mitral apparatus: annulus shape effect and chordal force distribution. Biomech Model Mechanobiol 2009;8(1):43-55.

[11] Liao J, Vesely I. A structural basis for the size-related mechanical properties of mitral valve chordae tendineae. J Biomech 2003;36:1125-1133.

[12] Dagum P, Timek TA, Green GR, Lai D, Daughters GT, Liang DH, Hayase M, Ingels NB, Miller DC. Coordinate-Free analysis of mitral valve dynamics in normal and ischemic hearts. Circulation 2000;102:III62-69.

[13] Timek T, Glasson JR, Dagum P, Green GR, Nistal JF, Komeda M, Daughters GT, Bolger AF, Foppiano LE, Ingels NB Jr, Miller DC. Ring annuloplasty prevents delayed leaflet coaptation and mitral regurgitation during acute left ventricular ischemia. J Thorac Cardiovasc Surg 2000;119:774-783.

Address for correspondence.
Dr Emiliano Votta
Dipartimento di Bioingegneria
Politecnico di Milano
Piazza L. da Vinci 32, 20133 Milano, Italy
E-mail: votta@biomed.polimi.it